Depolarized Dynamic Light Scattering from Diblock Copolymer Solutions Near the Order-Disorder Transition

Tao Jian, Spiros H. Anastasiadis,*,† and George Fytas

Foundation for Research and Technology—Hellas, Institute of Electronic Structure and Laser, P.O. Box 1527, 711 10 Heraklion, Crete, Greece

Keiichiro Adachi and Tadao Kotaka

Department of Macromolecular Science, Osaka University, Toyonaka, Osaka 560, Japan

Received March 4, 1993; Revised Manuscript Received May 12, 1993

ABSTRACT: Dynamic light scattering in the depolarized geometry has been used to investigate the behavior of solutions of an asymmetric diblock copolymer in a nonselective good solvent near the order-disorder transition (ODT), as a function of concentration, temperature, and scattering vector, q. A new q^2-dependent relaxation with q-dependent amplitude and depolarized intensity appears in the correlation function when the solution crosses from the disordered into the ordered state, which is accompanied by a significant increase in the depolarized intensity. This is attributed to the formation of grains of coherently-ordered long cylinders in the ordered state, with estimated coherence length of O (μm), that gives rise to a large form anisotropy in the microstructured solution. The coupled translational/rotational motion of these orientationally uncorrelated grains explains the observed diffusive relaxational dynamics.

Introduction

It has been recognized long ago that many experimental difficulties one encounters when investigating the rich variety and diversity of phase morphologies and the resulting phase transitions in diblock copolymers[1,2] are greatly alleviated when solvent is added to the melt. For a good solvent with roughly equal affinity for both blocks, the diblock copolymer solution is expected to exhibit thermodynamic effects similar to the undiluted melt. In such solutions the unfavorable interactions between the blocks are diluted by the solvent and, thus, the phase transitions may be more easily accessed for copolymers with relatively high molecular weights. Furthermore, equilibrium is more easily attained than in the melt. The effect of nonselective (neutral) solvents on the phase transitions in diblock copolymers has been investigated both experimentally[3-9] and theoretically.[10-14]

The ensemble of molecular configurations that produces the minimum overall free energy represents the equilibrium state of a block copolymer melt. The equilibrium phase morphology of a diblock copolymer, consisting of a contiguous linear sequence of polymerized monomers of species A covalently bonded to a second contiguous linear sequence of polymerized monomers of a different chemical species B, is determined by the overall number of segments, N, the overall volume fraction of segments A, f, and the Flory-Huggins interaction parameter $\chi = \chi_S + \chi_H/T$ with $\chi_H > 0$, χ_S constants, and T the absolute temperature. Due to both enthalpic and entropic contributions, it is the product χN that dictates the morphology for a certain f. By increasing N and/or lowering the temperature (increasing χ), an initially homogeneous melt undergoes a disorder-to-order transition[15-21] (ODT) toward a microphase characterized by a long-range coherent order in its composition. For even higher χN, highly organized periodic domain microstructures exist.[22-25] Seven types of ordered phase symmetries have been identified as a function of f: two types of body-centered-cubic spherical, two hexagonally-packed cylindrical, two types of an ordered-bicontinuous-double-diamond, and a lamellar morphology.

The early approach when investigating the behavior of diblock copolymer solutions was to adopt the "dilution" or "pseudobinary" approximation,[2,3,5,12] which states that the phase diagram of a copolymer solution in a nonselective solvent and its radiation scattering may be obtained by the corresponding melt phase diagram by replacing χ, the radius of gyration R_g, and the scattering power, $(a-b)^2$, by $\varphi\chi$, R_g, and $\varphi(a-b)^2$, respectively, where φ is the volume fraction of polymer in the solution. Careful examination of the validity of the pseudobinary approximation for both experimental and simulated data[5] showed that the approximation works better for the higher values of N, φ, and χ and for diblocks that deviate only slightly for the nonselectivity ($\chi_{AS} \approx \chi_{BS}$) and the "optical theta condition",[26] where χ_{KS} is the interaction parameter between block segment K and solvent. For high concentrations and/or low temperatures (high χ) a long-range coherent periodic microstructure has been obtained[2,3] with characteristic dimensions in agreement with mean-field strong-segregation theories of copolymer solutions;[11,23] for low concentration and/or high temperature homogeneous solutions have been observed[2,3] with the structure factor, $S(q)$, measured by small-angle X-ray scattering showing the characteristic correlation hole maximum[15] at a wave vector q^* independent of both φ and T and a magnitude increasing with increasing φ and/or decreasing temperature, similarly to the behavior of $S(q)$ of homogeneous diblock copolymer melts.

In this paper, we present the first depolarized dynamic light scattering investigation of the behavior of asymmetric diblock copolymer solutions in a nonselective solvent as a function of temperature and polymer concentration. A new relaxation process is observed at temperatures and/or concentrations just below the ODT. This process has a q^2-dependent relaxation rate and an amplitude and intensity that depend on q. The mode does not exist at temperatures and/or concentrations above the ODT. The appearance of the mode is accompanied by a significant increase in the depolarized light scattering intensity. We will show that these findings may be attributed to the development of large anisotropic "grains", i.e., regions in

* Author to whom correspondence should be addressed.
† Also at Physics Department, University of Crete, 71110 Heraklion Crete, Greece.

0024-9297/93/2226-4706$04.00/0

which the orientation of the microdomains is coherent, which result in a significant form of anisotropy in the microstructured solution. The dynamics observed is due to the diffusive motion of these grains that induce changes in the polarizability of the system.

Theoretical Background

Block Copolymer Solutions Near the ODT. The weak segregation limit (WSL) regime of diblock copolymer melts, $\chi N = O(10)$, encompasses the compositionally disordered phase and the various ordered phases very near the ODT. It is believed that, in the WSL, the ordered phases are not well-developed and that the individual polymers are slightly perturbed from their ideal Gaussian distribution. Leibler[15] provided an expression for the disordered-state scattering function and predicted the location of the ODT. This mean field approach predicts a stability limit at $(\chi N)_s = F(x^*,f)/2$, where $x = q^2R_g^2$, $R_g^2 = Nb^2/6$ is the mean-squared radius of gyration of the copolymer chain, b is the statistical segment length, the asterisk denotes the value at the peak of the structure fcator, i.e., at q^*, and $F(x^*,f)$ is a constant that depends on f. Fredrickson and co-workers[16,17] incorporated the order-parameter fluctuation corrections in the effective Hamiltonian for a diblock melt and found that the corrections are controlled by a Ginsburg parameter, $\bar{N}$, defined[16,21] by $\bar{N} = 6^3(R_g^3\rho_c)^2$, with ρ_c the chain number density, and predict a fluctuation-induced first-order transition at the ODT to occur at a lower temperature than the mean field stability limit, i.e., at[16]

$$(\chi N)_t = \frac{F(x^*,f)}{2} + \frac{2.0308}{2}[C(f)]^{2/3}(\bar{N})^{-1/3} \quad (1)$$

where $C(f)$ is a constant that depends on f.

Both the mean-field and the fluctuation theories have been extended[10-14] to treat the WSL of diblock copolymers in nonselective solvents good for both blocks by including (i) the nonclassical excluded-volume[13,14] effects to account for the deviation from mean-field behavior of polymer solutions due to local fluctuations in the solvent concentration, ψ_2 and (ii) the nonclassical effects[13,14] of local composition fluctuations of segments A and B, ψ_1. The excluded-volume effects, significant for the semidilute regime, were incorporated by using a treatment based on the blob theory,[27] whereas ψ_1 fluctuation effects were incorporated via the Hartree approximation.[16] It was predicted that the ODT for a block copolymer solution in a neutral solvent actually corresponds to a very narrow region of coexisting solvent-rich disordered and solvent-lean ordered phases. The dilution approximation was found to be an accurate approximation in the concentrated regime when used in conjunction with the Fredrickson–Helfand phase diagram,[16] i.e., the ODT is given by eq 1 when the interaction parameter χ is replaced with $\varphi\chi$. Therefore, for a certain N and f,

$$(\varphi\chi N)_t = \text{constant } C_1 \quad \text{(concentrated solutions)} \quad (2a)$$

For the important semidilute regime,[13,14] the blob model assumes that the copolymer chain in a good solvent consists of $Z = N\varphi^{1.31}$ blobs, with blob correlation length $\xi_b = b\varphi^{-0.77}$, that interact with a blob–blob interaction parameter $u \approx 0.67\chi\varphi^{0.29}$. The phase diagram is obtained by eq 1 when Z, u, and ξ_b are substituted instead of N, χ, and b. For a certain f and N, this leads to

$$(\varphi^{1.6}\chi N)_t = \text{constant } C_2 \quad \text{(semidilute solutions)} \quad (2b)$$

Dynamic Depolarized Rayleigh Scattering (DDRS). In quasi-elastic light scattering under homodyne conditions, the depolarized light scattering intensity autocorrelation function, $G_{VH}(q,t)$, is related to the desired normalized field correlation function, $g_{VH}(q,t)$, by

$$G_{VH}(q,t) = 1 + f^*|ag_{VH}(q,t)|^2 \quad (3)$$

where f^* is an experimental factor calculated by means of a standard and a is the fraction of $\langle I_{VH}(q,0)|\rangle$ with decay times slower than about 10^{-7} s. The field time correlation function may be written as[28]

$$g_{VH}(q,t) = \langle \sum_{j,k} \alpha_{yz}^k(t)\alpha_{yz}^j(0) \exp\{iq[r_k(t) - r_j(0)]\}\rangle / \langle|\delta\alpha_{yz}(q,0)|^2\rangle \quad (4)$$

where $\alpha_{yz}^k(t)$ is the yz component of the polarizability tensor of scattering element k, located at r_k at time t, in the laboratory fixed frame, $\langle ... \rangle$ denotes a statistical average, and $\delta\alpha_{yz}(q,0)$ is the polarizability density, $\delta\alpha_{yz}(q,0) = \sum_j \alpha_{yz}^j(0) \exp[iqr_j(0)]$. In this VH geometry, the incident laser beam propagates in the yz scattering plane with polarization parallel to the z-axis (V) and the scattered light is polarized parallel to the y-axis (H). The preexponential term is mainly affected by the reorientation of the scatterers, whereas the exponential term reflects the center of mass translational motion of the scattering elements.

For an assembly of cylindrical rods, the depolarized scattering intensity is related to the number density of particles, ρ, and the optical anisotropy of the particle, β, i.e, the anisotropic part of the polarizability, $\beta \equiv \gamma_\parallel - \gamma_\perp$, with subscripts $\parallel$ and $\perp$ denoting directions parallel and perpendicular to the cylinder axis, by

$$I_{VH}(q,t) = \frac{2\pi}{15}\rho\beta^2 F_{or}(t)F_{tr}(q,t) \quad (5)$$

with $F_{tr}(q,t)$ the translational part and $F_{or}(t)$ reflecting the orientational correlation function. For independent rotational and translational motion of small cylindrical scatterers, $F_{or}(t) = \exp(-6\Theta t)$, and $F_{tr}(q,t) = \exp(-q^2Dt)$, with Θ and D the rotational and translational diffusion coefficients. For asymmetric diffusion and/or rotational/translational coupling due to anisotropy in translational mobility, the expressions become much more complicated.[28,29] For the case of long rodlike scatterers with number density ρ_s and optical anisotropy β_s, the mean VH scattering intensity is[28]

$$I_{VH}(q,0) = \rho_s\beta_s^2\{{}^1/_2 Y(x_L) - {}^3/_4 X(x_L) - {}^1/_4 \cos\theta\, Z(x_L)\} = \rho_s\beta_s^2\Omega(x_L) \quad (6)$$

where $Y(x_L)$, $X(x_L)$, and $Z(x_L)$ are complicated functions of $x_L = qL$ and L is the length of the rod. For $x_L = O(1)$, i.e., for $L = O(1/q)$, $I_{VH}(q,0)$ depends strongly on q.

Aragón and Pecora[29] calculated the depolarized correlation function of long cylindrically symmetric, optically anisotropic rigid rods undergoing coupled rotational/translational motion. In the Rayleigh–Gans–Debye approximation,[28,29] $(4\pi/\lambda)L|n_A/n_B - 1| \ll 1$ (n_A and n_B are the refractive indices of the rods and their environment), they found that the VH scattering time autocorrelation function is an infinite series of decaying exponentials with time constants

$$\tau_{ml}^{-1} = q^2D + [l(l+1) + \omega_{ml}(p) - p/3]\Theta_\perp \quad m = 0, 1, 2;\ l = 0, 1, 2, ... \quad (7)$$

containing both the translational and rotational diffusion coefficients and spheroidal harmonic eigenvalues[29] ω_{ml}, which depend on the coupling parameter $p = q^2\Delta D/\Theta_\perp$,

where $\Delta D = D_{\parallel} - D_{\perp}$ is the anisotropy in the translational diffusion coefficient, $D = (D_{\parallel} + 2D_{\perp})/3$, and Θ is the rotational diffusion coefficient. The dynamical terms are weighted by structure factors that depend on p (i.e., on q). Numerical calculation[29] for $qL \approx 6$ at $\theta = 90°$ showed that experimentally one would not be able to resolve but only one time constant $\tau^{-1} = q^2D + \delta\Theta_{\perp}$, with the value of the p-dependent $\delta \sim 5.4$–6.3. According to eq 7, the relaxation rate τ^{-1} can be q-dependent if the translational part exceeds the rotational contribution, i.e., for large scatterers.

Experimental Section

Materials. An anionically synthesized poly(styrene-*b*-isoprene) diblock copolymer, denoted SI(43–86), was used. The details of its synthesis and characterization have been described earlier.[8,30] Its characteristics are as follows: total weight average molecular weight M_w = 129 000, polydispersity M_w/M_n = 1.06, 33.3% by weight polystyrene (PS). The synthetic procedure produced a polyisoprene (PI) sequence with cis:trans:vinyl ≈ 75:20:5. Using the average monomeric volume of PS and PI as a reference, N_{PS} = 480, N_{PI} = 1090, N = 1570, f_{PS} = 0.306, and $\bar{N}$ = 5000; the strong segregation limit equilibrium ordered morphology of this copolymer is a hexagonally-packed array of cylinders.[22–24] A relative low concentration (ca. 5% by weight) copolymer solution in toluene is initially prepared and filtered through a 0.22-μm Millipore filter directly into the dust-free light scattering cell (12.5 mm). During the measurements the cell was closed airtight to avoid evaporation of toluene. The concentration was checked before and after each measurement by weighing the solution. The concentration is then gradually increased by slow evaporation of small amount of solvent and reweighing the resulting solutions.

Photon Correlation Spectroscopy (PCS). The autocorrelation function of the depolarized light scattering intensity, $G_{VH}(q,t) = \langle I_{VH}(q,t)I_{VH}(q,0)\rangle/\langle|I_{VH}(q,0)|^2\rangle$, with $I_{VH}(q,0)$ being the mean light scattering intensity, is measured at different scattering angles, θ, using an ALV-5000 full digital correlator over the time range 10^{-6}–10^3 s. The incident beam from an Adlas diode pumped Nd-YAG laser, with wavelength λ = 532 nm and single mode intensity 160 mW, was polarized perpendicular (V) and the scattering beam parallel (H) to the scattering plane. $q = (4\pi n/\lambda)\sin(\theta/2)$ is the magnitude of the scattering vector, with n being the refractive index of the medium. The dual mode of the correlator was utilized in order to measure $G_{VH}(q,t)$ simultaneously for two different scattering angles. The desired field correlation function, $g_{VH}(q,t)$, is obtained from $G_{VH}(q,t)$ with eq 5. $g_{VH}(q,t)$ may be represented by single Kohlrausch–Williams–Watts (KWW) functions[28] $g_{VH}(q,t) = \exp[-(t/\tau)^{\beta_{KWW}}]$, where τ and β_{KWW} are respectively the KWW relaxation time and shape parameter.

Results

The normalized depolarized intensity correlation functions for a series of diblock copolymer solutions in toluene at $\theta = 90°$ scattering angle are shown in Figure 1a–d, with the traces of the corresponding normalized depolarized light scattering intensities, I^*, relative to the mean VH intensity of toluene shown as insets. At low concentrations, e.g., 10% by weight (Figure 1a) and up to 19 wt % (Figure 1b) and at 25 °C a completely flat correlation function is observed. No relaxation process is observed for these conditions with characteristic time in the time window of the correlator. Increasing, however, the concentration from 19 wt % to 21 wt % results in the appearance of a new relaxation process with characteristic time well within the time window of PCS, ca. 0.1 s. The process persists for lower and higher temperatures until the temperature reaches a characteristic value (for this concentration at 35 °C) when the process disappears. In Figure 1d, the correlation function is shown for 45 °C. Therefore, a new process appears in the depolarized correlation function of

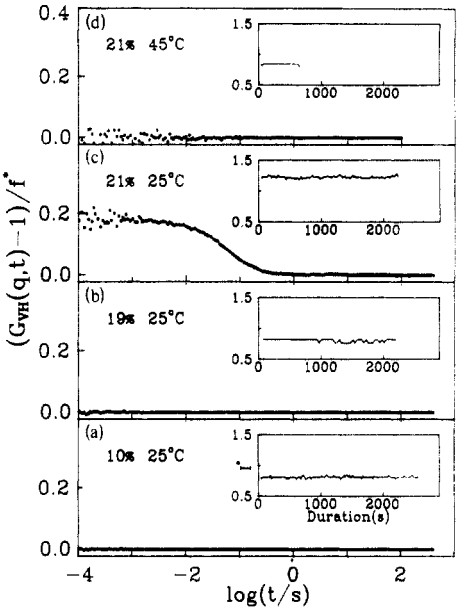

Figure 1. Depolarized intensity autocorrelation function for the SI(43-86)/toluene solution at $\theta = 90°$ scattering angle: (a) 10 wt % copolymer at 25 °C; (b) 19 wt % copolymer at 25 °C; (c) 21 wt % copolymer at 25 °C; (d) 21 wt % copolymer at 45 °C. The depolarized intensity normalized to the mean VH intensity of toluene trace with time is shown in the insets.

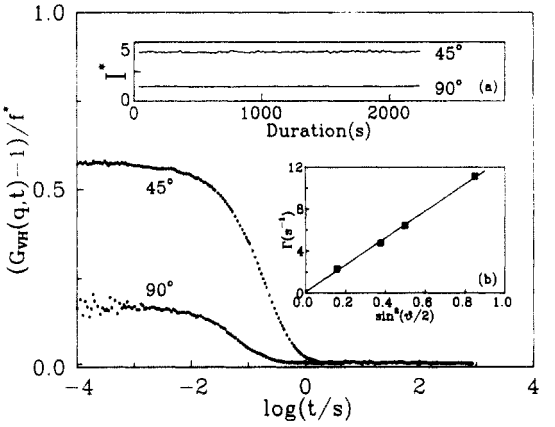

Figure 2. Depolarized intensity autocorrelation function for SI(43-86)/toluene solution (21 wt %) at 25 °C for two scattering angles, $\theta = 90°$ and $\theta = 45°$, recorded simultaneously with the dual mode of the correlator. The normalized depolarized intensity trace with time is shown in inset a, whereas the dependence of the relaxation rate on q^2 is shown in inset b.

asymmetric diblock copolymer solutions with increasing concentration that disappears with increasing temperature. This process is not related to local segmental orientation motion usually investigated by DDRS,[28] since for the copolymer solutions under investigation the segmental relaxation times are by many orders of magnitude faster and appear in the time window of PCS only at very low temperatures (below about −140 °C). Furthermore, the fact that the correlation function is found to be virtually single exponential ($\beta_{KWW} \approx 0.9$) supports the above statement.

The dependence of the new process on the scattering vector, q, is shown in Figure 2, where the correlation functions of the 21 wt % solution at 25 °C are shown for two different scattering angles of $\theta = 45°$ and 90°, with the traces of I^* in inset a. The relaxation rates of the process clearly depend on q and show a diffusive q^2 dependence in inset b. At the same time, both the mean normalized depolarized intensity and the amplitude of the correlation function depend strongly on q. We note here that when

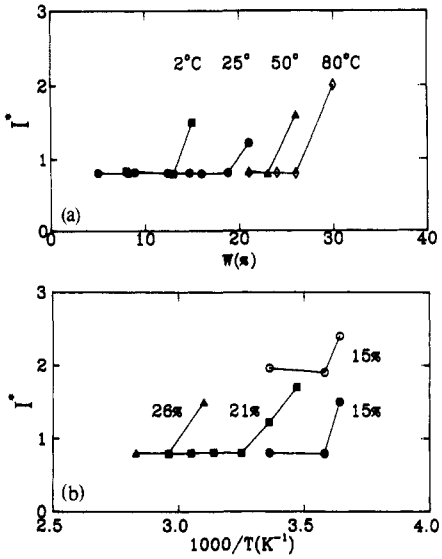

Figure 3. Mean depolarized light scattering intensity from SI-(43-86)/toluene solution at $\theta = 90°$ scattering angle, normalized to the mean depolarized intensity of toluene, as a function of (a) concentration for various temperatures (■, 2 °C; ●, 25 °C; ▲, 50 °C; ◇, 80 °C) and (b) temperature for various concentrations (▲, 26 wt %; ■, 21 wt %; ●, 15 wt %; ○, 15 wt % birefringence; see text). The lines are a guide to the eye.

the correlation function is featureless at 90° (as in Figure 1a,b,d), it is flat for all the angles investigated and its intensity is q-independent. The q-dependence of the relaxation time signifies a translational motion (the exponential term in eq 6) of anisotropic scattering elements over large distances of $O(1/q)$. The fact that the depolarized scattering intensity and amplitude of the depolarized correlation function depend on q shows that the size of the scatterers is at least $O(1/q)$. Note also that even at $\theta = 45°$ the short time intercept of the correlation function is less than 1. This means that a significant part ($1 - \sqrt{0.58} = 24\%$ at $\theta = 45°$) of the depolarized intensity relaxes with time constants faster than ca. 10^{-4} s. This relaxation is attributed to the fast segmental relaxations being outside the time window of PCS, discussed earlier.

Figure 3 shows the dependence of the mean polarized light scattering intensity at $\theta = 90°$ normalized to that of toluene at the same conditions on concentration for various temperatures (Figure 3a) and on temperature for various concentrations (Figure 3b). At low concentrations and/or high temperatures, the normalized VH intensity is low and almost independent of temperature and/or concentration. As the system crosses the characteristic temperature or concentration, the intensity increases rapidly. As is also shown in the insets of Figure 1a–d, the appearance and disappearance of the new depolarized mode is accompanied by a significant increase and decrease of the depolarized intensity, respectively.

Discussion

The preceding findings are consistent with the appearance of the new mode in depolarized light scattering corresponding to the disorder-to-order transition of the block copolymer solutions. For this system, the ODT leads from the disordered state to the formation of a spatially ordered phase with a hexagonally-packed array of cylinders of PS/toluene dispersed in a matrix of PI/toluene forming a "polydomain" or "polycrystalline" structure[31] composed of "grains". The orientations of the ordered cylinders are correlated within each domain, with orientational correlation length scale on the order of several microns (μm),[3,24,33–35] whereas there is no correlation between the different grains.[31,34] The oriented arrangement of the dimensionally anisotropic cylinders within each grain, with at least one dimension smaller than the wavelength of light, will result in significant optical anisotropy.[9,24,32,35] This can give rise to a measurable optical "form birefringence" in itself even without the involvement of molecular anisotropy.

Form birefringence has been observed a long time ago[24] in aligned single crystals of strongly phase-segregated poly(styrene-*b*-butadiene-*b*-styrene) triblocks ($N = 1100$, $f_{PS} = 0.2$) and recently in polycrystalline ordered samples of a melt of symmetric poly(styrene-*b*-methylmethacrylate)[32] ($N = 670$, $f_{PS} = 0.57$) and a SI/toluene microstructured solution[9] ($N = 400$, $f_{PS} = 0.4$). Actually, measurements of static birefringence were used to estimate the ODT for the last two systems,[9,32] in good agreement with rheological and small-angle scattering estimates of the ODT. A discontinuous decrease in the static birefringence of the sample upon heating was identified as the ODT.[9] This was also accompanied by a sharp decrease of the birefringent phase retardation and minimized light intensity.[32] The measured birefringence was attributed to the coherently-ordered grains present below the ODT, which disappear upon heating. We have measured the birefringence of our system by measuring the intensity of the light transmitted through the sample cell beam under cross-polarization (incident beam with V and transmitted beam with H polarization), similarly to ref 9, and the results are presented also in Figure 3b. An increase in the birefringence is observed for the 15 wt % solution at the same temperature where the new mode appears in VH scattering and where the depolarized scattering intensity increases abruptly. This is another verification that the appearance of the new depolarized mode is related to the formation of the long-range coherent cylindrical morphology.

In principle, there are two possible contributions to the static birefringence of each grain: form birefringence, due to the alternating domains, and intrinsic birefringence, due to both the orientation of the end-to-end vectors of the chains perpendicular to the microdomain interfaces and the stretching of the chains perpendicular to the interfaces. A theory to investigate the optical anisotropy of tethered chains in the strong segregation limit has recently appeared,[35] which provides expressions for the intrinsic contribution to the birefringence of a regular array of block copolymer cylinders, due to the orientation of the copolymer chains perpendicular to the interfaces and their extension, whereas the form birefringence of an assembly (grain) of parallel and similar "thin" cylindrical rods may be calculated according to basic principles of optics.[36,37]

The intrinsic polarizability anisotropy for a cylindrical morphology, i.e., the difference in the polarizability parallel and perpendicular to the axis of the cylinders, $\Delta\gamma_{in} = (\gamma_{\parallel} - \gamma_{\perp})_{in}$, is given by[35]

$$\Delta\gamma_{in} = -\frac{13\pi^2\rho_{cs}}{320}\left[(\alpha_1-\alpha_2)_A\frac{R_1^2}{\langle h_A^2\rangle_0} + \frac{48}{13\pi^2}(\alpha_1-\alpha_2)_B \times \ln\left(\frac{R_2}{R_1}\right)\left[\frac{R_2+R_1}{R_2-R_1}\frac{(R_2-R_1)^2}{\langle h_B^2\rangle_0}\right]\right] \quad (8)$$

where ρ_{cs} is the copolymer chain number density in the solution, and $\langle h_K^2\rangle_0$ is the mean-square unperturbed end-to-end distance of subchain K. R_1 denotes the radius of the inner cylinder containing the A block, and $2(R_2 - R_1)$ is the average thickness of the B layer in the matrix. They are related to the long period, L_c, of the cylindrical morphology by $R_1 = (f/\pi \sin 60)^{1/2}L_c$ and $R_2 = L_c/2 \sin 60$,

Table I. Molecular and Optical Constants of the Constituents

species	MW	m	σ (g/cm^3)	n	v_{seg} (Å^3/seg)	β^2 (Å^6)	$(\alpha_1-\alpha_2)_{LS}$ (Å^3)
PS	43000	104	1.05	1.59	164.4	38	-10.3
PI	86000	68	0.925	1.52	122.1	12	5.8
toluene		92	0.867	1.496	176.5	23	8.0

on the basis of simple geometrical arguments. For our SI(43-86)/toluene system the long period is estimated[2] to be L_c(21 wt %) = 650 Å, and R_1 = 220 Å and R_2 = 375 Å. $(\alpha_1 - \alpha_2)_K$ is the difference in the polarizabilities per segment along (α_1) and normal (α_2) to the chain backbone of a chain K, which may be estimated from the stress-optical coefficient[35] or, more appropriately in our case, from measurements of the optical anisotropy[38] per segment, β^2, which is related to $(\alpha_1 - \alpha_2)$ by[38] $\beta^2 = {}^9/_{25}(\alpha_1 - \alpha_2)^2$. The $\alpha_1 - \alpha_2$ values for the compounds of interest here are listed in Table I. The intrinsic anisotropy per chain is then $\Delta\gamma_{c,in} = \Delta\gamma_{in}/\rho_{cs}$.

The form birefringence, Δn_{form}, i.e., the difference in the refractive indices parallel and perpendicular to the array due to the assembly, depends solely on the volume fractions of the two microphases, F_A and F_B, and their respective refractive indices. Taking into account the electric displacement and the corresponding electric field inside the cylinders and in the space around them, Δn_{form} for a grain of parallel cylinders may be estimated as[36,37]

$$\Delta n_{form} = [F_A n_A^2 + F_B n_B^2]^{0.5} - n_B\left[\frac{(1+F_A)n_A^2 + F_B n_B^2}{(1+F_A)n_B^2 + F_B n_A^2}\right]^{0.5} \quad (9)$$

where n_K is the mean refractive index of medium K; i.e., the grain behaves as a positive uniaxial crystal with its optic axis parallel to the axes of the cylindrical rods. The mean scalar polarizability per scatterer, γ_s, with number density ρ_s is related to the mean refractive index, $\tilde{n}$, by the Lorentz–Lorentz expression[36]

$$\gamma_s = \frac{3}{4\pi\rho_s}\frac{\tilde{n}^2 - 1}{\tilde{n}^2 + 2} \quad (10)$$

Hence, the difference in the optical polarizabilities along the two principle axes (for small values of Δn) per scatterer (in this case per grain) is[36]

$$\Delta\gamma_s = \frac{9}{2\pi\rho_s}\frac{\tilde{n}}{(\tilde{n}^2+2)^2}\Delta n \quad (11)$$

Therefore, the polarizability anisotropy of the array of anisotropic scatterers (grain) is

$$\Delta\gamma_{form} = \frac{9}{2\pi}\frac{\tilde{n}}{(\tilde{n}^2+2)^2}\Delta n_{form} \quad (12)$$

and the anisotropy per grain is $\Delta\gamma_{s,form} = \Delta\gamma_{form}/\rho_s$.

The total depolarized intensity for the microstructured solution is due to (i) the intrinsic contribution due to the chain orientation, (ii) the form anisotropy due to the array of cylinders (grains), and (iii) the toluene solvent. The intrinsic contribution per chain and the form contribution per grain may be expressed in terms of the respective optical anisotropies, β, by[39] $\beta_{c,in}^2 = {}^9/_{25}(\Delta\gamma_{c,in})^2$ and $\beta_{s,form}^2 = {}^9/_{25}(\Delta\gamma_{s,form})^2$, similarly to the relationship between β^2 and $(\alpha_1-\alpha_2)^2$. The ratio of the VH intensity of the solution to that of toluene (Figures 1 and 3) is then

$$\frac{I_{VH,structured\ solution}}{I_{VH,toluene}} = \left(\frac{n_{tol}}{n_{solution}}\right)^2\left[\frac{\rho_{cs}\beta_{c,in}^2 + \rho_s\beta_{s,form}^2\Omega(X_L)}{\rho_{tol}\beta_{tol}^2} + (1-\varphi)\right] \quad (13)$$

whereas that for a homogeneous solution is

$$\frac{I_{VH,homogeneous\ solution}}{I_{VH,toluene}} = \left(\frac{n_{tol}}{n_{solution}}\right)^2\left[\frac{\rho_{PS}\beta_{PS}^2 + \rho_{PI}\beta_{PI}^2}{\rho_{tol}\beta_{tol}^2} + (1-\varphi)\right] \quad (14)$$

with ρ_{PS} and ρ_{PI} the segment number densities of PS and PI in solution, ρ_{tol} the number density of pure toluene, and n_{tol} and $n_{solution}$ the refractive indices.

The calculation is performed for the 21 wt % solution (φ = 0.19) at 90° ($q = 2.52 \times 10^{-3}$ Å^{-1}) using the refractive indices of Table I and calculating the average refractive indices as $n_{av} = \sum_i \varphi_i n_i$. The parameters involved are $\rho_{PS} = 4.8 \times 10^{-4}$ seg/Å^3, $\rho_{PI} = 1.1 \times 10^{-3}$ seg/Å^3, $\rho_{tol} = 5.7 \times 10^{-3}$ seg/Å^3, and $\rho_{cs} = 10^{-6}$ chains/Å^3. The mean refractive indices of the two microphases are n_A = 1.517 and n_B = 1.501, and their volume fractions are $F_A = 1 - F_B = 0.306$. The number density of grains, ρ_s, is related to the characteristic length of coherence of the ordered array by $\rho_s = L^{-3}$. Therefore, eqs 8–12 result in the following: $\Delta\gamma_{in} = 2.04 \times 10^{-6}$ (for the sample); $\Delta\gamma_{c,in}$ = 2.35 Å^3/chain, $\Delta n_{form} = 3.35 \times 10^{-5}$ (for the sample); $\Delta\gamma_{form} = 4.0 \times 10^{-6}$ (for the sample); $\Delta\gamma_{s,form} = (4.0 \times 10^{-6}/\rho_s)$ Å^3/grain. Then, a comparison between Figures 1 and 3 and eqs 13 and 14 and the form[29] of $\Omega(X_L)$ results in x_L = 19 and $L \approx 0.75$ μm, i.e., of the order of the reported coherence lengths.[3,24,32-34] The calculations also show that the form anisotropy contribution in eq 13 is much larger than the intrinsic anisotropy, due to the orientation of the chains perpendicular to the interfaces, and dominates the scattering. Therefore, the increase in the VH scattering intensity may be explained by the formation of grains of coherent hexagonally-packed cylinders with coherence length $L \approx 0.75$ μm. For these long scatterers, eq 8 results in a strongly q-dependent mean depolarized scattering intensity in agreement with experimental data.

Turning to the relaxational dynamics, the exponential form of the VH correlation function and the dependence of the relaxation rate on q^2 are in accord with eq 7, for concentration and/or temperature in the disordered state. For 21 wt % at 25 °C, the relaxation rate is dominated by the translational part, q^2D, with estimated $D = 1.7 \times 10^{-10}$ cm^2/s, since the rotational diffusion coefficient of these large, O (μm), objects is small. The featureless correlation function in the disordered state is due to the fact that the rotational diffusion of small particles (in this case segmental orientation) dominates the relaxation with rates much faster than the 10^{-6} s limit of PCS. The translational motion above the ODT is evident in the polarized light scattering correlation function.[6,7,40]

The order–disorder transition temperature and/or concentration of these diblock copolymer solutions may be understood in terms of the theory[13] discussed in the Introduction (eqs 1–4). Assuming $\chi = \chi_S + \chi_H/T$, eqs 4a,b become

$$\frac{1}{\varphi_{ODT}} = \frac{N\chi_S}{C_1} + \frac{N\chi_H}{C_1}\frac{1}{T_{ODT}} \quad \text{(concentrated solutions)} \quad (15a)$$

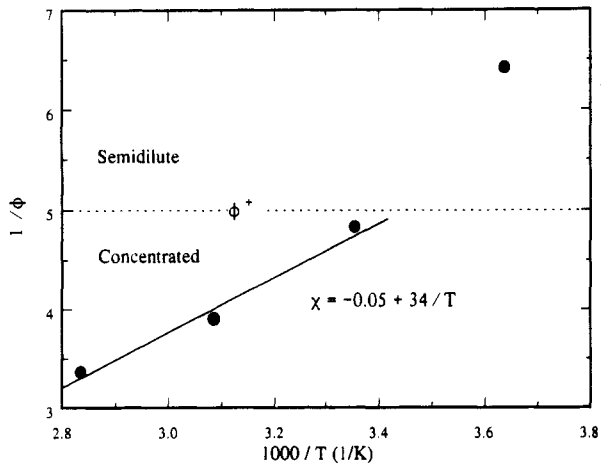

Figure 4. Inverse of the copolymer volume fraction in solution versus the inverse of temperature at the ODT. The solid line is a fit to eq 2a for the three higher concentrations. The dashed line denotes the crossover concentration between the semidilute and the concentrated regimes.

$$\frac{1}{\varphi_{ODT}^{1.6}} = \frac{N\chi_S}{C_2} + \frac{N\chi_H}{C_2}\frac{1}{T_{ODT}} \quad \text{(semidilute solutions)} \tag{15b}$$

with C_1 calculated as[13] $C_1 = 19.34$, whereas the calculation of C_2 from theory is inadequate due to the very low values of $Z = N\varphi^{1.31}$. The ODT data are shown in Figure 4 using the representation of eq 15a. For the three highest concentrations, the data result in $\chi = 0.05 + 34/T$, on the basis of the average monomeric volume, in agreement with literature values.[5,9,20] At the low concentration of $\varphi_{ODT} = 0.156$, the solution exists in the semidilute regime (the crossover concentration from semidilute to concentrated is estimated[27] to be $\varphi^+ = 0.20$) and the system should obey eq 15b.

In summary, we have demonstrated that the ODT in diblock copolymer solutions is accompanied by the appearance of a new relaxation process in the depolarized light scattering intensity correlation function. This mode exhibits a q^2-dependent relaxation rate and an amplitude that depends on q. These findings are consistent with the formation of coherently ordered cylindrical domains ("grains") with coherence length of the O (μm), which result in significant optical anisotropy, and q-dependent relaxation rates and intensity. We note, however, that this process has not been reported before for diblock copolymer melts when investigating their segmental relaxations in VH scattering.[41] The process should appear at time scales much slower than the segmental relaxation process, and its existence for melts is currently under investigation. However, a significant increase in the VH scattering intensity in a poly(dimethylsiloxane-*b*-methylethylsiloxane) diblock copolymer melt with very small molecular optical anisotropy has been observed below temperatures near the ODT and its origin is being explored.[42]

References and Notes

(1) Bates, F. S.; Fredrickson, G. H. *Annu. Rev. Phys. Chem.* **1990**, *41*, 525. Bates, F. S. *Science* **1991**, *251*, 898.
(2) Hashimoto, T. In *Thermoplastic Elastomers*; Legge, N. R., Holden, G., Schroeder, H. E., Eds.; Hamser: Vienna, 1987.
(3) Hashimoto, T.; Shibayama, M.; Kawai, H. *Macromolecules* **1983**, *16*, 1093. Shibayama, M.; Hashimoto, T.; Hasegawa, H.; Kawai, H. *Macromolecules* **1983**, *16*, 1427. Hashimoto, T.; Kowasaka, K.; Shibayama, M.; Kawai, H. *Macromolecules* **1986**, *19*, 754.
(4) Pico, E. R.; Williams, M. C. *J. Appl. Polym. Sci.* **1987**, *22*, 445.
(5) Hashimoto, T.; Mori, K. *Macromolecules* **1990**, *23*, 5347.
(6) Balsara, N. P.; Stepanek, P.; Lodge, T. P.; Tirrell, M. *Macromolecules* **1991**, *24*, 6227.
(7) Balsara, N. P.; Eastman, C. E.; Foster, M. D.; Lodge, T. P.; Tirrell, M. *Makromol. Chem. Macromol. Symp.* **1991**, *45*, 213.
(8) Yao, M.-L.; Watanabe, H.; Adachi, K.; Kotaka, T. *Macromolecules* **1992**, *25*, 1699.
(9) Balsara, N. P.; Perahia, D.; Safinya, C. R.; Tirrell, M.; Lodge, T. P. *Macromolecules* **1992**, *25*, 3896.
(10) Benmouna, M.; Benoit, H. *J. Polym. Sci., Polym. Phys. Ed.* **1983**, *21*, 1227. Benoit, H.; Wu, W.; Benmouna, M.; Mozer, B.; Bauer, B.; Lapp, A. *Macromolecules* **1985**, *18*, 986.
(11) Hong, K. M.; Noolandi, J. *Macromolecules* **1983**, *16*, 1083.
(12) Onuki, A.; Hashimoto, T. *Macromolecules* **1989**, *22*, 879.
(13) Fredrickson, G. H.; Leibler, L. *Macromolecules* **1989**, *22*, 1238.
(14) Olvera de la Cruz, M. *J. Chem. Phys.* **1989**, *90*, 1995.
(15) Leibler, L. *Macromolecules* **1980**, *13*, 1602.
(16) Fredrickson, G. H.; Helfand, E. *J. Chem. Phys.* **1987**, *87*, 697.
(17) Barrat, J. L.; Fredrickson, G. H. *J. Chem. Phys.* **1991**, *95*, 1282.
(18) Olvera de la Cruz, M. *Phys. Rev. Lett.* **1991**, *67*, 85.
(19) Mori, K.; Hasegawa, H.; Hashimoto, T. *Polym. J.* **1985**, *17*, 799. Mori, K.; Tanaka, H.; Hasegawa, H.; Hashimoto, T. *Polymer* **1989**, *30*, 1389.
(20) Owens, J. N.; Gancarz, I. S.; Koberstein, J. T.; Russell, T. P. *Macromolecules* **1989**, *22*, 3380.
(21) Bates, F. S.; Rosedale, J. H.; Fredrickson, G. H. *J. Chem. Phys.* **1990**, *92*, 6255.
(22) Helfand, E.; Wasserman, Z. R. In *Development of Block Copolymers I*; Goodman, I., Ed.; Applied Science: London, 1982.
(23) Meier, D. J. In *Thermoplastic Elastomers*; Legge, N. R., Holden, G., Schroeder, H. E., Eds.; Hamser: Vienna, 1987.
(24) Keller, A.; Odell, J. A. In *Processing, Structure and Properties of Block Copolymers*; Folkes, M. J., Ed.; Elsevier: New York, 1985. Folkes, M. J.; Keller, A. *Polymer* **1971**, *12*, 222.
(25) Thomas, E. L.; Alward, D. B.; Kinning, D. J.; Handlin, D. L.; Fetters, L. J. *Macromolecules* **1986**, *19*, 2197. Hasegawa, H.; Tanaka, H.; Yamasaki, K.; Hashimoto, T. *Macromolecules* **1987**, *20*, 1651.
(26) Fukuda, T.; Nagata, M.; Inagaki, H. *Macromolecules* **1984**, *17*, 548.
(27) de Gennes, P. G. *Scaling Concepts in Polymer Physics*; Cornell University Press: Ithaca, NY, 1979.
(28) Berne, B. J.; Pecora, R. *Dynamic Light Scattering*; Wiley-Interscience: New York, 1976. Pecora, R., Ed. *Dynamic Light Scattering. Applications of Photon Correlation Spectroscopy*; Plenum Press: New York, 1985.
(29) Aragón, S. R.; Pecora, R. *J. Chem. Phys.* **1985**, *82*, 5346.
(30) Yao, M.-L.; Watanabe, H.; Adachi, K.; Kotaka, T. *Macromolecules* **1991**, *24*, 2955.
(31) Hashimoto, T. *J. Appl. Polym. Sci.: Appl. Polym. Symp.* **1985**, *41*, 83.
(32) Amundson, K.; Helfand, E.; Patel, S. S.; Quan, X.; Smith, S. D. *Macromolecules* **1992**, *25*, 1935.
(33) Ehlich, D.; Takenaka, M.; Hashimoto, T. *Macromolecules* **1993**, *26*, 492.
(34) Hashimoto, T.; Nagatoshi, K.; Todod, A.; Hasegawa, H.; Kawai, H. *Macromolecules* **1974**, *7*, 364.
(35) Lodge, T. P.; Fredrickson, G. H. *Macromolecules* **1992**, *25*, 5643.
(36) Born, M.; Wolf, E. *Principles of Optics*; Pergamon Press: New York, 1970.
(37) Wiener, O. *Abh. Sachs. Ges. Akad. Wiss., Math.-Phys. Kl. No. 6* **1912**, *32*, 575.
(38) Fytas, G.; Floudas, G.; Hadjichristidis, N. *Polym. Commun.* **1988**, *29*, 322. Saiz, E.; Floudas, G.; Fytas, G. *Macromolecules* **1991**, *24*, 5796.
(39) Flory, P. G. *Statistical Mechanics of Chain Molecules*: Wiley-Interscience: New York, 1969.
(40) Jian, T.; Anastasiadis, S. H.; Adachi, K.; Kotaka, T. Manuscript in preparation.
(41) Rizos, A. K.; Fytas, G., Roovers, J. E. L. *J. Chem. Phys.* **1992**, *97*, 6925. Anastasiadis, S. H.; Fytas, G.; Vogt, S.; Gerharz, B.; Fischer, E. W. *Europhys. Lett.* **1993**, *22*, 619.
(42) Vogt, S.; Anastasiadis, S. H.; Fytas, G. Unpublished data.